University of Utah
UNDERGRADUATE RESEARCH JOURNAL

COMPARATIVE ANATOMY AND CONNECTIVITY OF THE AII AMACRINE CELL IN MOUSE AND RABBIT RETINA

Selena Wirthlin, Bryan W. Jones, Crystal L. Sigulinsky, James R. Anderson, Daniel P. Emrich, Christopher N. Rapp, Jeebika Dahal, Rebecca L. Pfeiffer, Kevin D. Rapp, Jia-Hui Yang, Carl B. Watt, Robert E. Marc
Department of Ophthalmology and Visual Sciences

Purpose:

Studying the comparative retinal anatomy of different models relevant to vision research is important for understanding how we develop therapies and cures for blinding diseases. Mouse retina structurally differs from rabbit retina, as it is thicker and vascularized, while the rabbit retina is thinner and avascular. The implications of these differences on neuronal morphology and connectivity is not yet known. This project compares the morphology and connectivity of the Aii amacrine cell (AC) with ultrastructural precision in connectomes of rabbit (RC1) and mouse (RC2) retina. The Aii amacrine cell is a crucial cell class required for night vision and involved in the switching between retinal networks from bright to dark environments and vice versa.

Methods:

RC1 and RC2 are retinal connectomes built by automated transmission electron microscopy at ultrastructural (2 nm/pixel) resolution. RC1 and RC2 are 0.25mm diameter volumes of retina. RC1 is from a 13-month-old, female Dutch Belted rabbit. RC2 is from a 5-month-old female C57BL/6J mouse. The Viking application was used to annotate Aii cells and all of the chemical and electrical synapses formed by these cells in both connectomes. The specific quantities of each synapse type were counted using the Cell Sketches software. Through these applications, data was derived from 3 rabbit Aii ACs (cells 514, 2610, 3679) and 1 mouse Aii AC (cell 5106). 2 additional mouse Aii ACs (cells 5922 and 6171) are partially annotated but are not included in the quantification analyses.

The presence of some synapses, such as gap junctions, can be difficult to visualize and confirm due to small size or non-optimal angle but in some instances that can be solved by doing a recapture. Figure 1 shows a recapture that was performed to confirm the identity of 2 synapses in question. In Figures 1B and 1C, we see two gap junctions, G1 and G2, at a 0° tilt and 20° tilt, respectively. The identity of a gap junction can be confirmed by the pentalaminar structure which appears as alternating dark-light-dark-light-dark bands within the synapse. This structure can be observed for G1 (Figure 2B') without any additional tilt. However, in order to observe the pentalaminar structure of G2, a tilt of 20° was needed (Figure 2C'). The recapture validated the identity of the gap junctions.

Results:

Aii ACs are axonless, narrow-field, glycinergic interneurons that stratify throughout the inner plexiform layer (IPL) of the retina (Kolb and Famiglietti, 1974; Strettoi et al., 1992; Tsukamoto and Omi, 2013; Marc et al., 2014). The morphology of mouse and rabbit Aii amacrine cells aligns with the anatomical structure of the retina in each species. The mouse Aii ACs are noticeably elongated to span the thicker inner plexiform layer and have prominent neck and waist regions (Figure 2A). The rabbit Aii ACs span a thinner inner plexiform layer and are more compact, lacking distinct neck and waist regions (Figure 2A). The arboreal dendrites of rabbit Aii ACs travel obliquely through the ON sublamina, while those of mouse Aii ACs travel more vertically with limited lateral expansion until they reach the bottom half of the ON sublamina, which coincides with the terminals of rod bipolar cells (RBCs) (middle panel, Figure 1B). RC1 is from mid-peripheral retina and it is therefore unclear whether some of the lateral expansion of rabbit Aii AC dendrites is due to eccentricity.

Mouse Aii ACs exhibit distinct synaptic compartments, largely corresponding with the stratification of their principle synaptic partners (Figure 2B). Lobular dendrites in the OFF sublamina are dominated by conventional pre-synapses with OFF cone bipolar cells (CBC) and post-synaptic densities to their reciprocal ribbon pre-synapses. Gap junctions with ON cone bipolar cells and other Aii cells are largely restricted to the ON sublamina and dominate the arboreal dendrites in the waist region while post-synaptic densities to RBC ribbon synapses dominate deeper in the arboreal dendrites. In rabbit Aii ACs the conventional pre-synapses and gap junctions occupy distinct compartments, namely the OFF versus ON sublamina, respectively (Figure 2C). However, the post-synaptic densities and gap junctions in the ON sublamina are less compartmentalized in the rabbit than in the mouse (left panel, Figure 2C). The locations of these post synaptic densities are consistent with the location of the interactions between the rabbit Aii and RBCs and the difference can be attributed to the greater lateral spread of RBC axonal terminals in the rabbit retina, at least in this region (middle panels, Figure 2B,C). Mouse cell 5106 was found to form gap junctions with the descending axons of ON CBCs as they pass both its soma and lobular dendrites (arrows, right panel, Figure 2B). This finding is notable as gap junctions were not found in these locations in rabbit Aii ACs (right panel, Figure 2C). The structure of the mouse and rabbit inner nuclear layer differs between mouse and rabbit, with mouse exhibiting 2-3 layers of stacked cell somas, while rabbit exhibits 1.5 layers. In both species, somas of Aii cells are positioned at the bottom of this layer, and the lack of gap junctions between rabbit CBC axons and Aii somas may simply be due to not having the opportunity to interact and form those synapses.

While the locations of these synaptic components were fairly consistent between the rabbit and mouse Aii ACs, the frequency of these synapses between species did vary (Table 1). The synaptic components were quantified from 1 mouse Aii AC (cell 5106) and 3 rabbit Aii ACs (cells 514, 2610, and 3679). These preliminary comparisons suggest that the mouse Aii AC has far more total synaptic interactions than rabbit Aii ACs. The mouse Aii AC exhibits approximately twice the number of conventional pre-synapses and about one and a half times the number of postsynaptic densities and gap junctions compared to rabbit Aii ACs. Despite these differences in synaptic frequencies, the overall input to output ratio is similar between species.

However, the data suggests that mouse Aii AC's have more output in the OFF sublamina as compared to the ON sublamina, suggesting a possible difference in Aii output to the ON versus OFF pathways of the retina between species. Evaluation of this will require the partners to be classified.

In an attempt to further expand the sample size and allow for a more accurate comparison between mouse and rabbit, 2 additional mouse Aii ACs (5922 and 6171) have been partially annotated in the RC2 connectome (Figure 3). While incomplete, these cells do exhibit synaptic distributions and ratios that align with that of 5106 and support its general connectivity trends. The morphology of cells 5922 and 6171 also follows suit of the completed cell 5106, with the exception of a unique morphological difference observed for cell 5922. As shown in Figure 4, a large branch originates from the lobular dendrites and travels down vertically to terminate in the inner plexiform layer with few synaptic connections.

The unique branch of cell 5922 is similar to AIS-like segments discussed in previous literature (Wu et al., 2011; Tsukamoto and Omi, 2013). Axon-bearing neurons possess an axon initiating segment (AIS) where action potentials originate. The Aii AC is an axonless neuron but appears to have an AIS-like segment depicted as a unique dendritic process, that supports spiking activity (Wu et al., 2011). The AIS-like segment of cell 5922 in this study originated from the lobular dendrites and traveled down, terminating in the OFF sublamina of the IPL while making only two synapses. This morphology and connectivity resemble the findings of AIS-like segments described previously (Wu et al., 2011; Tsukamoto and Omi, 2013), as morphology and synaptology of AIS-like segments can greatly vary. These previously described AIS-like segments all originate from the lobular dendrites and may travel downwards to terminate in the ON or OFF sublamina of the IPL *or* travel obliquely upward and terminate in the inner nuclear layer (INL). Some AIS-like segments make few post-synaptic densities while others frequently make conventional and gap junction synapses. Previous data suggests that conventional pre-synapses are likely present due to evidence of potential glycine release (Wu et al., 2011), and the AIS-like segment of cell 5922 does make a conventional pre-synapse, like several of those described by Tsukamoto and Omi (2013).

Tsukamoto and Omi (2013) describe additional features of AIS-like segments in mouse Aii AC's. They describe an undercoating of dense granular material that appears intermittently for the duration of the AIS-like segment. In the AIS-like segment of cell 5922, a strikingly similar intermittent undercoating of granular material was observed (Figure 5). This density is an important feature in identifying the AIS-like segment because of the variability in morphology and synaptology of the AIS-like segment of Aii cells and will be used to look for an AIS-like segment in the other mouse Aii cells and to determine if it is also present in rabbit Aii cells.

Conclusions:

Clear morphological and connectivity differences exist between mouse and rabbit Aii ACs. Noticeable morphological differences unique to mouse Aii ACs may be due to increased retinal thickness and stratification differences in partner cells, although lateral expansion of rabbit Aii ACs may be partially attributable to eccentricity. These morphological differences may affect connectivity. The layering of somas in the inner nuclear layer may influence the locations of gap

junctions and signal flow between Aii cells and ON CBCs. Preliminary assessment of gap junction partners suggested lower connectivity between Aii cells for the mouse Aii as compared to the rabbit. The reduced lateral spread by arboreal dendrites of mouse Aii ACs may not allow the cell an opportunity to gap junction with itself or as many other Aii ACs like the laterally extending arboreal dendrites of rabbit Aii ACs, which would increase the relevant output to the ON sublamina and potentially normalize the OFF:ON output ratio between mouse and rabbit Aii ACs. Future work will identify the synaptic partners of these rabbit and mouse Aii cells to allow a better evaluation of connectivity differences between these species. While certain characteristics of the AIS-like segments differ between previous reports (Wu et al., 2011; Tsukamoto and Omi, 2013) and this study, the morphological and synaptic similarities between them allows for a common feature set for identifying these unique processes of Aii ACs and their identification across species. The role these AIS-like segments play is not fully understood and further research should be done to investigate whether the AIS-like segment is to an axonless neuron as the AIS is to an axon-bearing neuron in terms of initiation of action potentials, neuron excitability, and cell communication. As additional Aii cells and their partners continue to be flushed out, the similarities and differences in morphology and connectivity will become more apparent and allow for a more comprehensive comparison of the Aii AC between species. Comparative anatomy connectomics is essential for understanding possible implications of retinal structure on neuronal morphology and connectivity that may underlie network differences between the mouse and rabbit retina.

Support:

This work was supported by the University of Utah Office of Undergraduate Research, NIH grants R01 Grant EY02576, R01 EY028927, R01 EY015128, T32 EY024234, P30 EY014800, and an Unrestricted Grant from Research to Prevent Blindness to the Department of Ophthalmology and Visual Sciences.

References:

Kolb H, Famiglietti EV (1974) Rod and cone pathways in the inner plexiform layer of cat retina. Science 186:47-49.

Marc RE, Anderson JR, Jones BW, Sigulinsky CL, Lauritzen JS (2014) The AII amacrine cell connectome: a dense network hub. Frontiers in neural circuits 8:104.

Strettoi E, Raviola E, Dacheux RF (1992) Synaptic connections of the narrow-field, bistratified rod amacrine cell (AII) in the rabbit retina. The Journal of comparative neurology 325:152-168.

Tsukamoto Y, Omi N (2013) Functional allocation of synaptic contacts in microcircuits from rods via rod bipolar to AII amacrine cells in the mouse retina. The Journal of comparative neurology 521:3541-3555.

Wu C, Ivanova E, Cui J, Lu Q, Pan ZH (2011) Action potential generation at an axon initial segment-like process in the axonless retinal AII amacrine cell. The Journal of neuroscience : the official journal of the Society for Neuroscience 31:14654-14659.

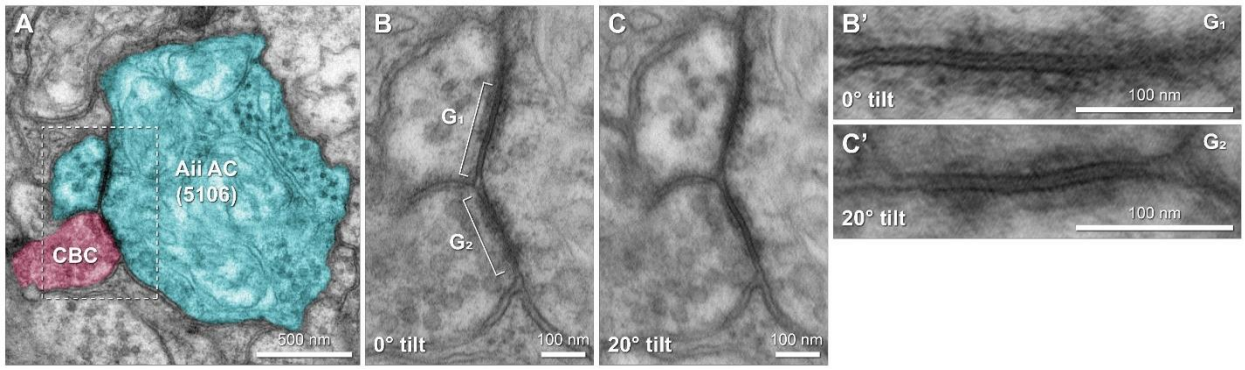

Figure 1: Recapture of gap junction for validation. (A) Candidate gap junctions identified at native 2.18 nm/pixel resolution in connectome RC1 between mouse Aii AC 5106 (teal) with another branch of itself (teal, top, G_1) and an ON cone bipolar cell (pink, bottom, G_2). (B-C) Recapture of boxed region in A at 30,000 X magnification (0.36 nm/pixel) with goniometric tilts of 0° (B) and 20° (C) used to confirm gap junction identity of G_1, and G_2, respectively. (B',C') enlarged to view pentalaminar structure characteristic of gap junctions. Scale bar: (A) 500 nm; (B, B', C, C') 100 nm. Abbreviations: CBC, cone bipolar cell; G, gap junction.

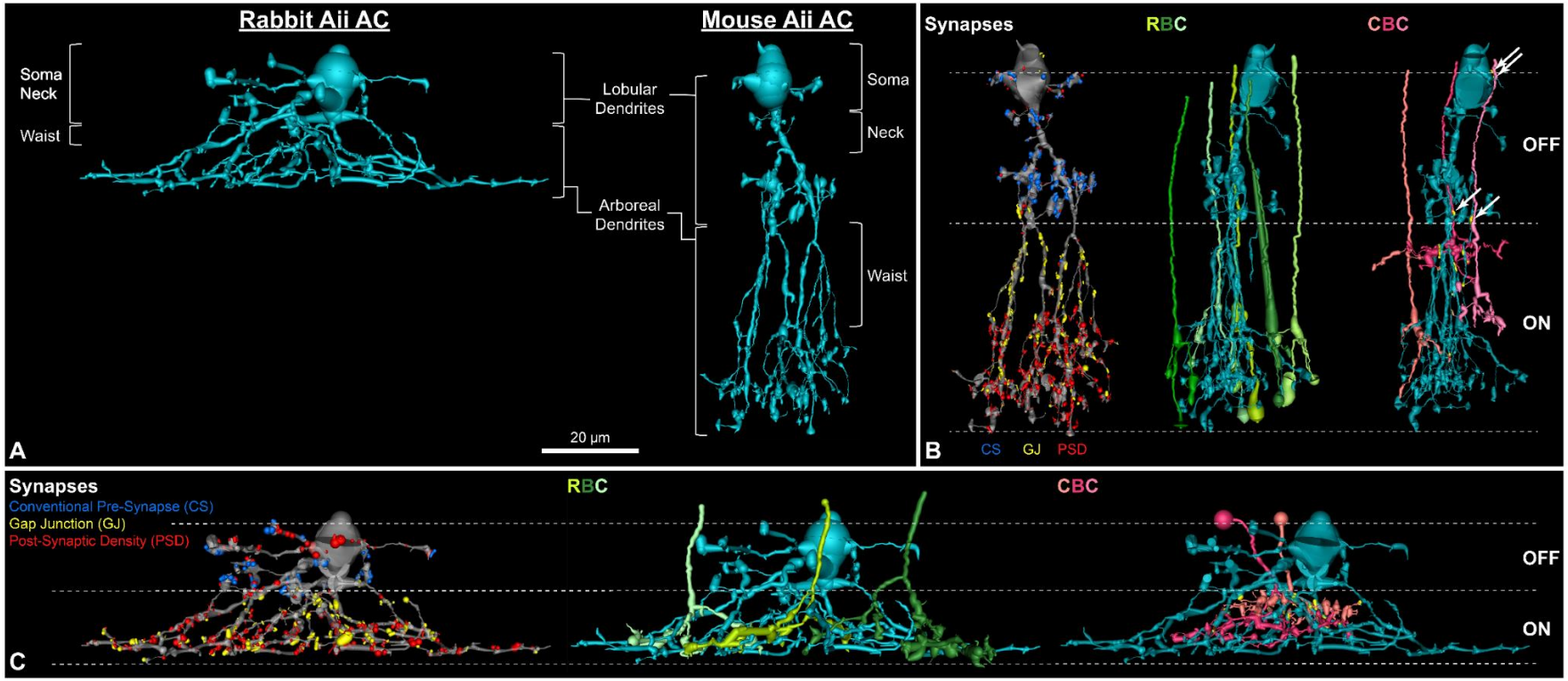

Figure 2: Comparison of morphology and synaptology of Aii amacrine cells between mouse and rabbit. (A) A side-by-side comparison of the variations observed in overall and region specific morphology between the rabbit and mouse Aii ACs. (B) Mouse Aii AC synaptic components (left panel) and interacting RBCs (center panel) and CBCs (right panel). Synaptic components are color coded according to the key in (C): conventional pre-synapses (blue), post-synaptic densities (red), and gap junctions (yellow). White arrows represent the location of gap junctions unique to the mouse Aii AC. (C) Rabbit Aii AC synaptic components (left panel) and interacting RBCs (middle panel) and CBCs (right panel). Scale bar: 20µm. Abbreviations: CBC, cone bipolar cell, RBC, rod bipolar cell.

Feature	Rabbit (Mean ± SD, *n* = 3)	Mouse (Aii AC 5106)
Total conventional pre-synapses	55.4 ± 15	124
Total gap junctions	104.8 ± 13.7	148
Total post-synaptic densities	272.4 ± 39.1	442
[a]Input : Output	2.3 : 1	2.2 : 1
[b]Output to OFF : ON	0.53 : 1	0.83 : 1

Table 1: Comparisons of connectivity across species. Frequency of synaptic components and calculation of network contributions based on 3 rabbit Aii ACs (cells X, Y, and Z) and 1 mouse Aii AC (cell 5106).

[a]Input reflect the sum of gap junctions and post-synaptic densities. Output reflects the sum of gap junctions and conventional pre-synapses.

[b]Output to OFF pathways approximated as the frequency of conventional pre-synapses. Output to ON pathways approximated as the frequency of gap junctions.

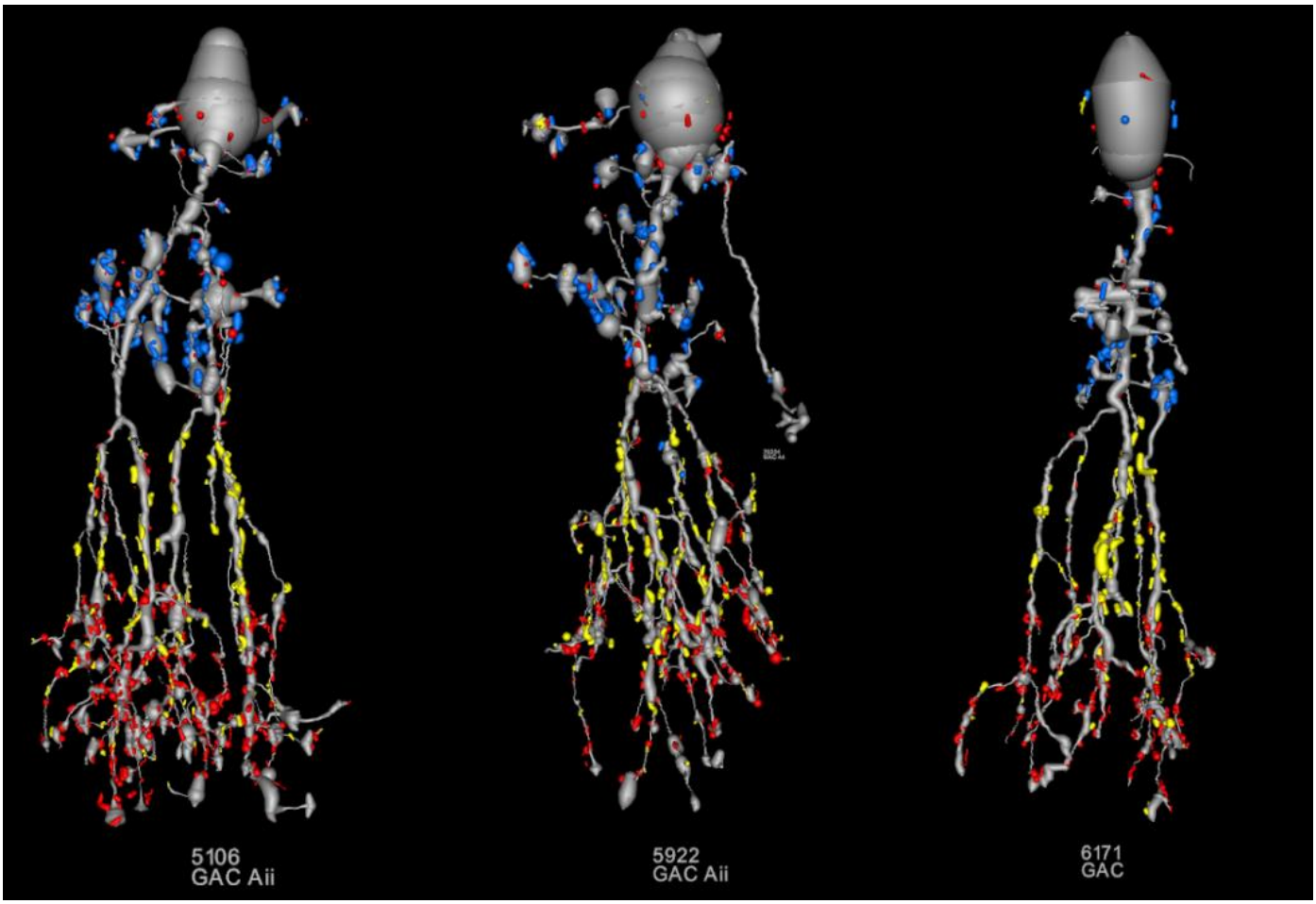

Figure 3: Three Aii ACs from mouse retina. Cell 5106 is completely annotated. Cells 5922 and 6171 are partially annotated. The morphology and synaptology of all follow what is expected from an Aii AC. Synaptic components are color coded as follows: conventional pre-synapses (blue), post-synaptic densities (red), and gap junctions (yellow).

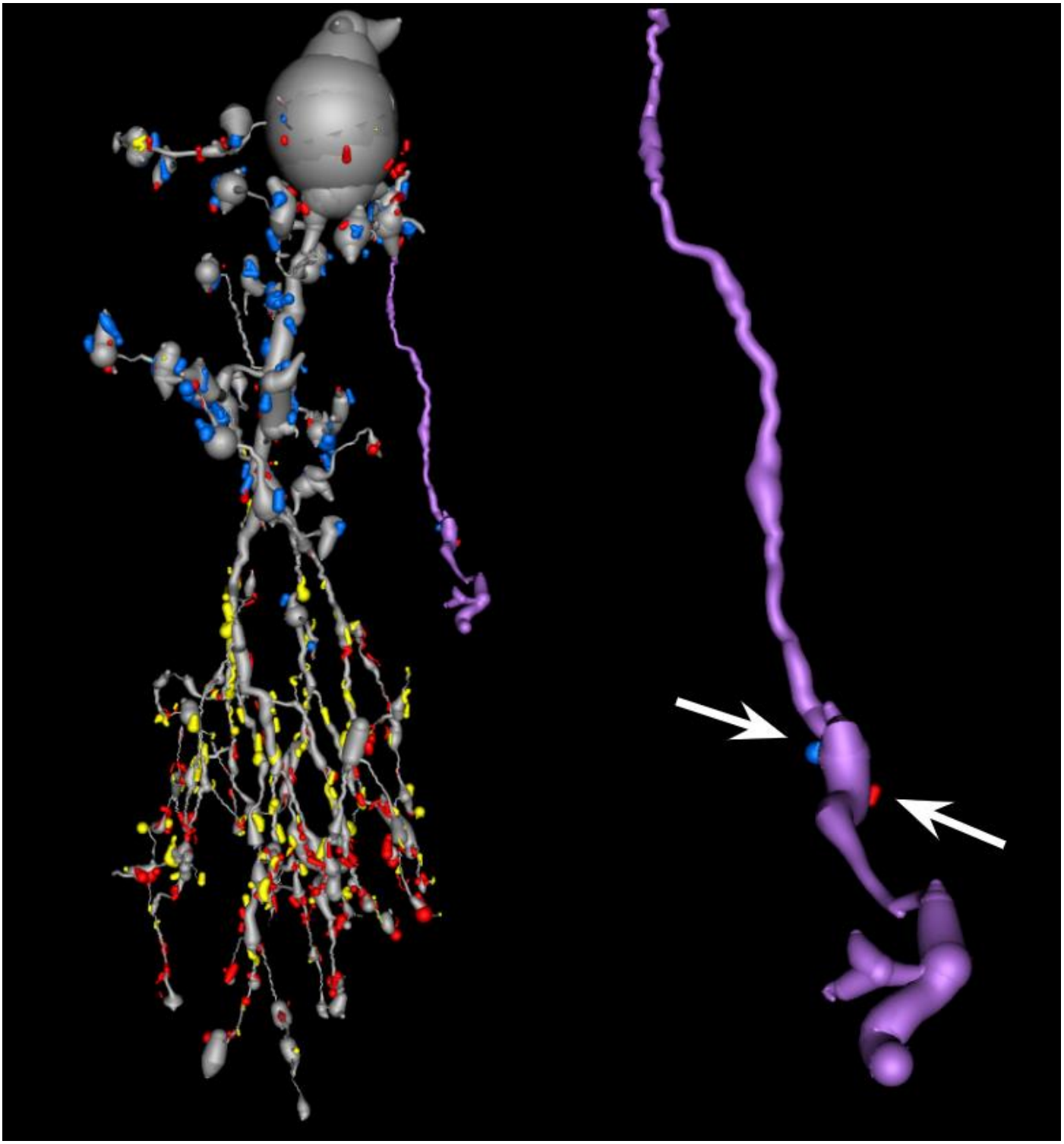

Figure 4: AIS-like segment of cell 5922. The AIS-like segment is shown in purple in contrast to the rest of the cell (gray) and zoomed in on the right. This segment makes minimal synapses (white arrows). Synaptic components are color coded as follows: conventional pre-synapses (blue), post-synaptic densities (red), and gap junctions (yellow).

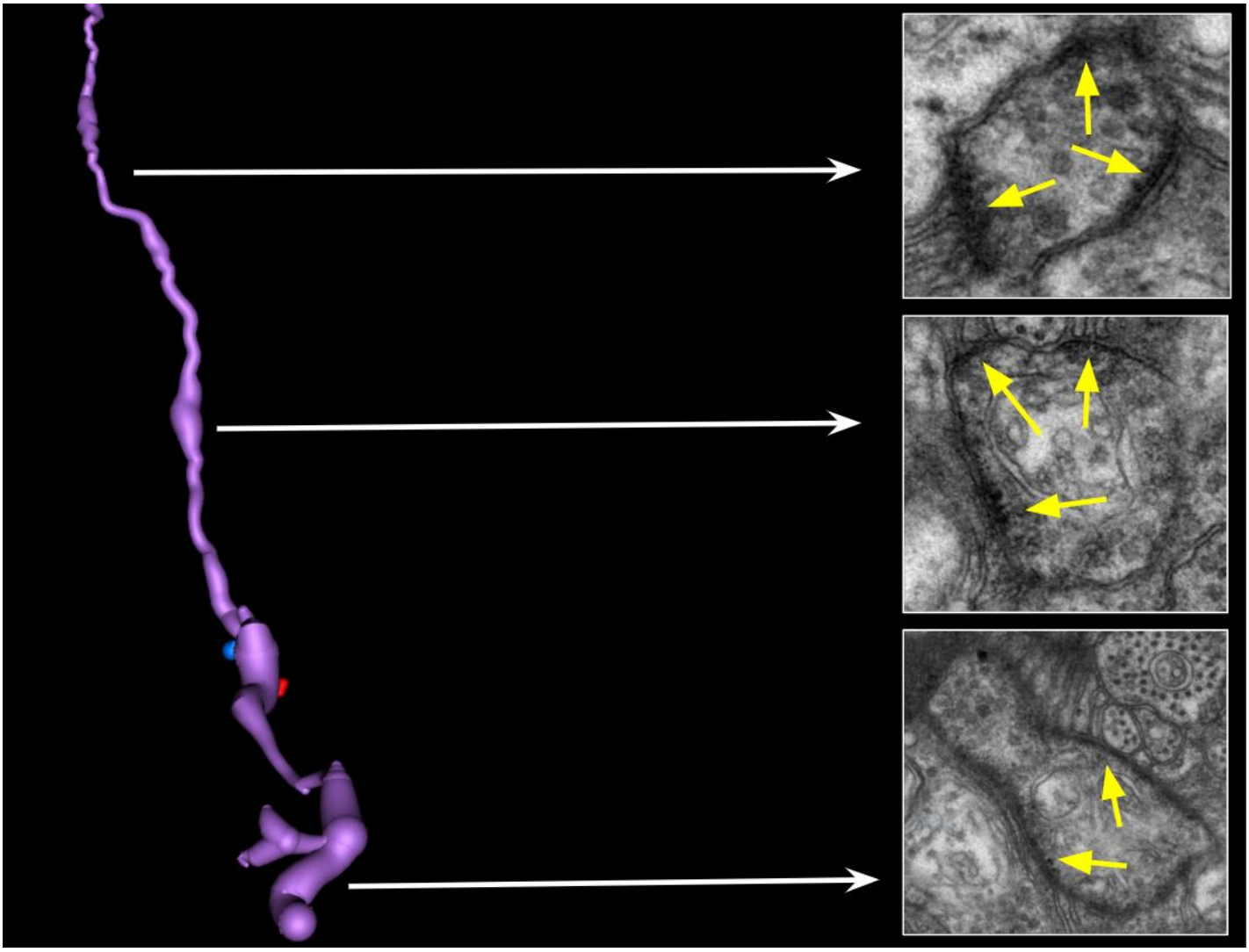

Figure 5: Dense granular undercoat found in the AIS-like segment of cell 5922. The undercoat of dense granular material found in cell 5922 was found intermittently throughout the AIS-like segment. Yellow arrows show the densities found in these locations.